Environmental Forensics, 12:342–348, 2011

ISSN: 1527–5922 print / 1527–5930 online
DOI: 10.1080/15275922.2011.622347

Taylor & Francis
Taylor & Francis Group

Recent Changes in Atmospheric Polycyclic Aromatic Hydrocarbons (PAHs) and Nitropolycyclic Aromatic Hydrocarbons (NPAHs) in Shenyang, China

Ning Tang,[1] Takahiro Tokuda,[1] Akihiko Izzaki,[1] Kenji Tamura,[2] Ruonan Ji,[3] Xuemei Zhang,[3] Lijun Dong,[3] Takayuki Kameda,[1] Akira Toriba,[1] and Kazuichi Hayakawa[1]

[1]*Graduate School of Natural Science and Technology, and Institute of Medical, Pharmaceutical and Health Sciences, Kanazawa University, Kanazawa, Japan*
[2]*National Institute for Environmental Studies, Tsukuba, Japan*
[3]*Division of Science & Education, Shenyang Center for Disease Control and Prevention, Shenyang, China*

Airborne particulates were collected in three size fractions by using Anderson low-volume air samplers in Shenyang, China, in winter and summer in 2007. Compared with data obtained in 2001 at the same sites, the total concentrations of nine polycyclic aromatic hydrocarbons (PAHs) in winter decreased by 67% at one site and decreased by 40% at the other site, while the total concentrations of four nitropolycyclic aromatic hydrocarbons (NPAHs) did not decrease. This suggests that environmental countermeasures begun in 2001 were effective in decreasing the concentration of PAHs. However, in summer, the concentrations of PAHs and NPAHs rose by the factors of 4 and 5, respectively, possibly because of an increase in the number of motor vehicles.

Keywords: polycyclic aromatic hydrocarbon (PAH), nitropolycyclic aromatic hydrocarbon (NPAH), 1-nitropyrene/pyrene ratio ([1-NP]/[Pyr]), air pollution, Shenyang government Blue Sky Project

Many polycyclic aromatic hydrocarbons (PAHs) and nitropolycyclic aromatic hydrocarbons (NPAHs) are carcinogenic and/or mutagenic. The International Agency for Research on Cancer (IARC). has ranked benzo[*a*]pyrene (BaP) in Group 1 (carcinogenic to humans) and 1-nitropyrene (1-NP) in Group 2A (probably carcinogenic to humans) (IARC, 2005). Several PAHs also have estrogenic/antiestrogenic or antiandrogenic activities (Kizu et al., 2000). Atmospheric PAHs such as BaP and NPAHs such as 1-NP mainly originate from imperfect combustion and pyrolysis of organic matters (Hayakawa et al., 1995a; Rogge et al., 1993). In addition, some NPAHs, such as 2-NP, are formed in the atmosphere via reactions of their parent PAHs and NO_2 (Arey et al., 1986). We previously reported that the main contributors to atmospheric PAHs and NPAHs were automobiles in Japanese and South Korean commercial cities (Sapporo, Kanazawa, Toyama, Tokyo and Seoul) (Kakimoto et al., 2000; 2002; Hayakawa et al., 2000; 2002; Tang et al., 2002a; 2005), while they were coal combustion systems in Chinese and Far-eastern Russian cities (Beijing, Shenyang, Fushun, Tieling and Vladivostok) (Hattori et al., 2007; Hayakawa et al., 2007; Tang et al., 2002a; 2005; 2009).

During the past three decades, large increases in the consumption of petroleum and coal in China have led to air pollution. In Shenyang, a city that is the economic center of northeast China, the main sources of air pollution are exhausts from domestic heating, industry, and motor vehicles. In Shenyang in 2001 to 2002, the average concentrations of total PAHs (nine types of PAHs) and NPAHs (seven types of NPAHs) were 534 pmol m^{-3} and 677 fmol m^{-3}, respectively (Hattori et al., 2007). These concentrations were significantly higher than those in Kanazawa, Japan in the same period. To reduce air pollution, the Shenyang government undertook the Blue Sky Project (Shenyang Environmental Protection Bureau of China [SYEPB]), in which 100 factories were transferred to the outer city, and 5,000 inefficient boilers for domestic heating were removed from 2001 to 2007. These changes helped to reduce the annual average concentrations of PM_{10} from 190 μg m^{-3} in 2001 to 120 μg m^{-3} in 2009 (SYEPB).

In this study, airborne particulates (APs) were collected by using the same method and at the same sites as our previous investigation in 2007 (Hattori et al., 2007). Our objectives were to clarify the effect of the above countermeasures and to understand the present pollution status of PAHs and NPAHs in Shenyang, China.

Address correspondence to Ning Tang, Graduate School of Natural Science and Technology, and Institute of Medical, Pharmaceutical and Health Sciences, Kanazawa University, Kakuma-machi, Kanazawa 920-1192, Japan. E-mail: tou@p.kanazawa-u.ac.jp

Materials and Methods

Sampling Sites

Sampling sites in this study were the same as our previous study (Hattori et al., 2007). SY-1 (Heping Elementary School) was in a commercial area and SY-2 (Taishan Elementary School) was in a mixed residential and commercial area. Airborne particulates were collected simultaneously at the two sites using Andersen low-volume air samplers (AN-200, Shibata Sci. Tech., Tokyo, Japan) at a flow rate of 28.3 L min^{-1}. The height of the intake varied from 1 to 3 m above ground level. APs were separately collected only in three fractions according to their aerodynamic size: >7 μm, 2.1–7 μm, and <2.1 μm onto quartz fiber filters (2500QAT-UP, Pallflex Products, Putnam, CT,USA), which differed from our previous study (Hattori et al., 2007; APs were collected in nine fractions and separated in same three granulometric groups for PAHs and NPAHs analysis). Air samples were collected at two sites on March 10–17 (winter) and September 17–24, 2007 (summer). Filters were replaced daily. At each site, seven three-layer filters were used for each of the above sampling periods. The filters were dried in a desiccator in the dark, weighed and stored at −20°C until use.

Chemicals

USEPA 610 PAHs mix, a mixture of 16 PAHs including fluoranthene (FR), pyrene (Pyr), benz[*a*]anthracene (BaA), chrysene (Chr), benzo[*b*]fluoranthene (BbF), benzo[*k*]fluoranthene (BkF), BaP, benzo[*ghi*]perylene (BgPe) and indeno[1,2,3-*cd*]pyrene (IDP) were purchased from Supelco Park (Bellefonte, PA, USA). Two internal standards for PAHs (pyrene-d_{10} (Pyr-d_{10}) and benzo[*a*]pyrene-d_{12} (BaP-d_{12})) were purchased from Wako Pure Chemicals (Osaka, Japan). 1-NP, 6-nitrochrysene (6-NChr), 6-nitrobenzo[*a*]pyrene (6-NBaP) and an internal standard for NPAHs (2-fluoro-7-nitrofluorene (FNF)) were purchased from Chiron AS (Trondheim, Norway). All other chemicals used were of analytical reagent grade.

Sample Treatment and Analytical Procedures

Three-layer filters (>7 μm, 2.1–7 μm, <2.1 μm) of each sample were cut into small pieces and placed in a flask, respectively. By this treatment, the concentrations of PAHs and NPAHs in the three groups were obtained for each sample. Both PAHs and NPAHs were extracted ultrasonically twice with benzene/ethanol (3:1, v/v) and then the solution was filtered with a 0.45 μm membrane filter (HLC-DISK13, Kanto Chemical Co., Inc., Tokyo, Japan). Internal standards, Pyr-d_{10}, BaP-d_{12} and FNF, were added to the flask prior to the ultrasonic extraction. In the case of PAHs, the filtrate was evaporated to dryness. The residue was dissolved in 0.5 mL of acetonitrile, and then injected into the HPLC system for PAHs. In the case of NPAHs, the filtrate was washed once with 5% (w/v) sodium hydroxide solution, once with 20% (v/v) sulfuric acid solution, and twice with water for removing acid and base substance. Then the solution was evaporated to dryness with rotation evaporator. The residue was dissolved in 1 mL of 75% ethanol-0.02 M acetic acid-sodium acetate buffer (pH 5.5). The solution was filtered with a 0.45 μm HLC-Disk membrane filter (Kanto Chemical Co., Inc., Tokyo, Japan), and an aliquot of this solution was injected into the HPLC system for NPAHs. Other conditions were the same as in our previous reports (Hayakawa et al., 1991; Tang et al., 2002b).

The nine PAH species were determined by using HPLC with fluorescence detection. The PAH HPLC system consisted of a reversed-phase column (Inertsil ODS-P, 4.6 i.d. × 250 mm, GL Sciences Inc., Tokyo, Japan) with an acetonitrile/water gradient and fluorescence detection. The flow rate was 1 mL/min^{-1}. The time program of the fluorescence detector was set to detect at the optimum excitation and emission wavelengths for each PAH. Other conditions were the same as in our previous report (Tang et al., 2002b).

The four NPAH species were determined by using HPLC with chemiluminescence detection. The HPLC system consisted of two reversed-phase columns (Cosmosil 5C18-MS, 4.6 i.d. × (250 + 150) mm, Nacalai Tesque, Tokyo, Japan) connected in series with chemiluminescence detection. The mobile phase was 10 mM imidazole buffer (pH 7.6)-acetonitrile (1:1, v/v), and the chemiluminescence reagent solution was an acetonitrile solution containing 0.02 mM bis(2,4,6-trichlorophenly)oxalate and 15 mM hydrogen peroxide. The flow rate was 1 mL min^{-1} for each solution. Other conditions were the same as in our previous report (Hayakawa et al., 1991; Tang et al., 2003).

Data Analysis

The major sources of PAHs and NPAHs were identified by a cluster analysis with Ward's method and standardized squared Euclidean distance. The statistical analysis software program used in this study was kindly provided by Dr. Susumu Hayakari of Aomori Prefectural Institute of Public Health and Environment (Aomori, Japan). For the cluster analysis, we used the concentration ratios of 1-NP to Pyr, 6-NBaP to BaP and individual PAH to total PAHs in the airborne particulates collected at two sites in 2001 – 2002 (Hattori et al., 2007) and 2007. The data of Tokyo in summer in 2004 and in winter in 2005 were used grouping (Tang et al., 2005). The data of average temperature, dew point and wind speed in Shenyang during our sampling periods were obtained from USA National Climatic Data Center (2009) and average humidity were calculated by using the data of average temperature and dew point.

Results and Discussion

Concentrations

The PAH and NPAH concentrations were higher in winter than in summer at each site and they were both higher at SY-1 than

Table 1. *Atmospheric concentrations of nine polycyclic aromatic hydrocarbons (PAHs) and four nitropolycyclic aromatic hydrocarbons (NPAHs) in 2007 at two sites in Shenyang, China*

		Summer		Winter	
		SY-1	SY-2	SY-1	SY-2
PAH	FR	7.97 ± 3.55	7.22 ± 3.33	67.9 ± 36.0	51.6 ± 26.7
(pmol m^{-3})	Pyr	6.99 ± 2.60	6.41 ± 2.63	70.1 ± 34.8	60.3 ± 31.8
	BaA	7.11 ± 3.63	5.41 ± 2.94	63.1 ± 28.2	57.9 ± 35.2
	Chr	13.4 ± 7.52	9.91 ± 6.19	79.8 ± 34.3	67.5 ± 34.0
	BbF	34.3 ± 28.5	28.7 ± 27.9	69.9 ± 32.9	61.8 ± 32.4
	BkF	11.2 ± 8.66	9.71 ± 8.62	26.5 ± 11.9	24.9 ± 12.6
	BaP	11.4 ± 6.45	10.2 ± 6.70	44.1 ± 19.3	42.9 ± 22.1
	BgPe	24.6 ± 13.8	23.1 ± 14.9	46.0 ± 17.1	56.2 ± 26.5
	IDP	14.4 ± 8.57	14.6 ± 10.0	22.2 ± 9.24	27.5 ± 13.1
	Total PAHs	131 ± 80.2	115 ± 79.6	491 ± 215	451 ± 226
NPAH	9-NA	718 ± 400	600 ± 369	5400 ± 3280	5430 ± 3210
(fmol m^{-3})	1-NP	159 ± 49.8	147 ± 54.7	857 ± 459	555 ± 184
	6-NC	205 ± 100	191 ± 86.0	544 ± 260	343 ± 157
	6-NBaP	31.9 ± 15.6	32.4 ± 14.6	116 ± 58.5	93.4 ± 64.1
	Total NPAHs	1110 ± 526	972 ± 493	6910 ± 3450	6420 ± 3410

All data represent mean±standard deviation; $n = 7$.

at SY-2 (Table 1). Measurements made in 2001 to 2002 showed similar increases in winter (Hattori et al., 2007).

Figure 1 compares the total concentrations of nine PAHs and three NPAHs measured in the two studies (One of NPAHs measured in the present study was not measured in the earlier study). In winter, the concentrations of PAHs decreased by 40% at SY-1, which is in a commercial area, and decreased by 67% at SY-2, which is in a more residential area (Figure 1A). However, the concentration of NPAHs did not change markedly at either site, which suggests that Shenyang's Blue Sky Project was more effective against PAHs than NPAHs in winter. In summer, the concentrations of PAHs and NPAHs rose by a factor of at least 4 at both sites. A likely contributing factor was an increase in the number of motor vehicles from 360,000 in 2000 to 560,000 in 2007 ((SYEPB).

Distribution of PAHs, NPAHs and APs in Different Size Particulate Fractions

The concentrations and compositions of air pollution matters are often affected by meteorological conditions (Yamasaki et al., 1982). PAH, NPAH and AP concentrations were found to be highly correlated with humidity at the two sites in summer (Table 2). However, no such correlations were found with temperature or wind speed, possibly because of their smaller ranges (15–22°C and 1.3–2.4 m s^{-1}) and because rainfall was only one-third the normal amount during the summer sampling period. However, in winter, AP (>7 μm) was negatively correlated with humidity and positively correlated with wind speed at both sites. Temperature also seemed to be positively correlated with PAH and NPAH levels in all size fractions. These observations suggest that cold and dry air, which blows predominantly from the inner Asian continent in winter, increased the concentrations of coarse particulates (>2.1 μm) and decreased the concentrations of PAHs, NPAHs and fine particulates (<2.1 μm) in the atmosphere (Table 2).

The main sources of atmospheric PAHs and/or NPAHs in Shenyang in summer are automobiles, while in winter they seem to be coal stoves and coal boilers used for domestic heating (Tang et al., 2005; Hattori et al., 2007; Kong et al., 2010). In 2007, the percentages of total PAHs and NPAHs in the fine particulate fraction, which is the fraction that most adversely

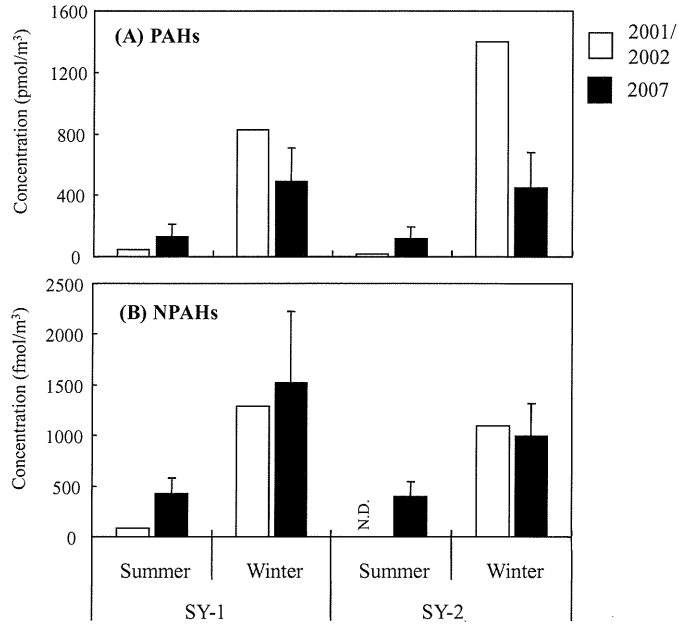

Figure 1. Graph for comparison of atmospheric polycyclic aromatic hydrocarbons (PAHs) and nitropolycyclic aromatic hydrocarbons (NPAHs) at two sites in Shenyang in 2001–2002 and in 2007. Each bar means the average concentration of total PAHs or NPAHs; PAHs includes FR, Pyr, BaA, Chr, BbF, BkF, BaP, BgPe and IDP; NPAHs includes 1-NP, 6-NC and 6-NBaP. The data of Shenyang in 2001 –2002 are from Hattori et al. (2007).

Table 2. Correlation coefficients between polycyclic aromatic hydrocarbons (PAHs), nitropolycyclic aromatic hydrocarbons (NPAHs), and airborne particulates (APs) in different particulate fractions and several meteorological conditions

		Winter			Summer		
		Temperature (°C)	Wind speed (m s^{-1})	Humidity (%)	Temperature (°C)	Wind speed (m s^{-1})	Humidity (%)
Meteorological Condition	Wind speed (m s^{-1})	−0.58			−0.71		
	Humidity (%)	0.27	−0.81*		−0.63	0.19	
SY-1	PAHs (>7 μm)	0.24	−0.64	0.79*	*0.20	0.12	−0.83**
	PAHs (7 − 2.1 μm)	0.54	−0.74	0.82**	0.04	0.31	−0.75*
	PAHs (<2.1 μm)	0.43	−0.81*	0.92**	−0.11	0.56	−0.63
	NPAHs (>7 μm)	0.41	−0.47	0.37	0.18	−0.18	−0.73
	NPAHs (7 − 2.1 μm)	0.61	−0.65	0.50	0.03	−0.02	−0.67
	NPAHs (<2.1 μm)	0.27	−0.63	0.70	0.13	0.18	−0.82**
	APs (>7 μm)	−0.49	0.90**	−0.84**	0.04	−0.04	−0.63
	APs (7− 2.1 μm)	−0.11	0.70	−0.58	−0.05	−0.04	−0.55
	APs (<2.1 μm)	0.76	−0.64	0.57	−0.20	0.14	−0.49
SY-2	PAHs (>7 μm)	0.48	−0.81*	0.83**	0.21	0.07	−0.84**
	PAHs (7 − 2.1 μm)	0.62	−0.77*	0.61	0.09	0.17	−0.76*
	PAHs (<2.1 μm)	0.34	−0.77*	0.79*	−0.14	0.57	−0.52
	NPAHs (>7 μm)	0.42	−0.75*	0.73	0.34	0.05	−0.88**
	NPAHs (7 − 2.1 μm)	0.66	−0.92**	0.76*	0.16	0.21	−0.79*
	NPAHs (<2.1 μm)	0.63	−0.87**	0.79*	0.18	0.10	−0.86**
	APs (>7 μm)	−0.39	0.90**	−0.90**	0.47	−0.21	−0.90**
	APs (7 − 2.1 μm)	−0.00	0.50	−0.62	0.18	0.01	−0.79*
	APs (<2.1 μm)	0.68	−0.66	0.53	−0.04	0.19	−0.61

$n = 7$. The data of average temperature, dew point and wind speed in Shenyang during the sampling periods were obtained from National Climatic Data Center (2009) and average humidity were calculated by using the data of average temperature and dew point.

affects human health, were about 92% and 81%, respectively at both sites (Figure 2), in agreement with previous reports. (Hayakawa et al., 1995b; Kawanaka et al., 2004). However, in 2002, the percentages of total PAHs and total NPAHs in the fine fraction were 70% and 60% of the total, respectively. In winter 2002, the coarse size particulates had high PAH and NPAH levels (Figure 2). In general, inefficient boilers contributed greatly to the large size particulates in the atmosphere because of their imperfect combustion. Therefore, the increase in the ratio of the total PAHs and total NPAHs in the fine fraction from 2002 to 2007 was probably due to the removal of approximately 5000 boilers by the Shenyang government.

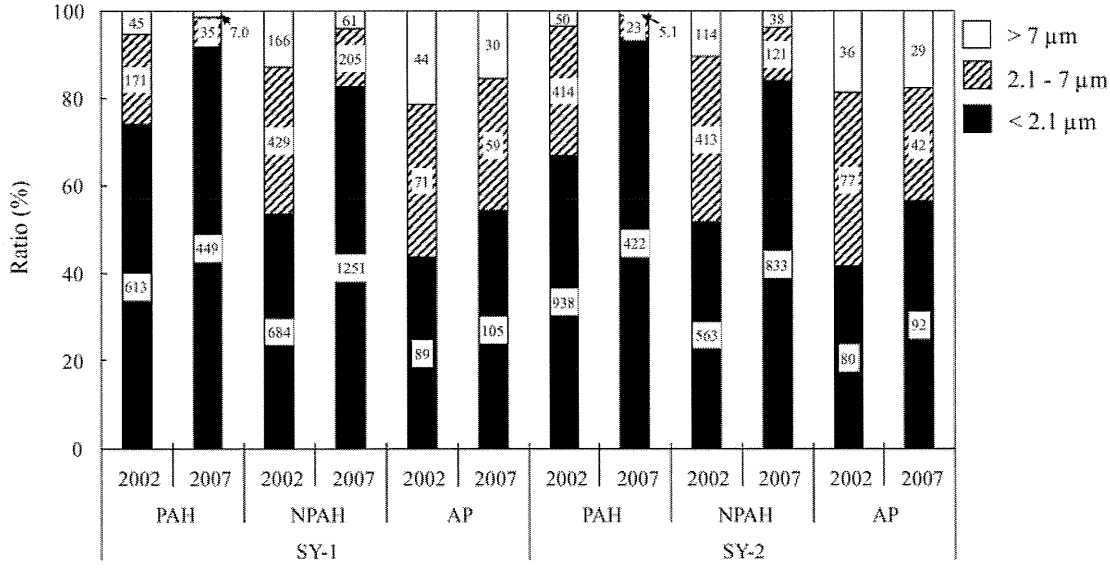

Figure 2. Graph of particulate partitions of polycyclic aromatic hydrocarbons (PAHs), nitropolycyclic aromatic hydrocarbons (NPAHs), and airborne particulates (APs) in three size fractions at two sites in Shenyang in 2001–2002 and in 2007. Three size fractions mean larger 7 μm, 7 − 2.1 μm and smaller than 2.1 μm. The data of Shenyang in 2001–2002 are referenced from Hattori et al. (2007). The concentrations of PAHs, NPAHs and APs in each particulate size fraction are shown within each box.

However, the difference of atmospheric concentrations of NPAHs between 2002 and 2007 was not significant. According to our previous study, the concentrations of NPAHs in the particulates collected in automobiles were significantly higher than those in coal combustion systems. By contrast, the concentrations of PAHs were lower in automobiles (Hayakawa et al., 2000; Tang et al., 2005). In addition, the particulate sizes originating from automobiles were very small (Ho et al., 2006). These observations suggest that the increase in the number of motor vehicles also contributed to the fine particulate fractions of PAHs and NPAHs, especially the latter.

Compositions and Main Sources

Multivariate statistical analysis methods and several diagnostic ratios have been used to identify possible emission sources of PAHs and NPAHs and to compare their compositions in the atmosphere (Bourotte et al., 2005; Kakimoto et al., 2002; Rogge et al., 1993). The compositions of PAHs and NPAHs were compared by a cluster analysis using Ward's method. As parameters, we used the concentration ratios of 1-NP to Pyr, 6-NBaP to BaP and individual PAHs to total PAHs in the airborne particulates collected at the two sites in 2001–2002 and 2007. The same compound pairs were investigated in Tokyo in summer in 2004 and in winter in 2005 (Tang et al., 2005) and are used here as a reference. As shown in Figure 3, two large clusters were observed according to the compositions of PAHs and NPAHs at all sites. Cluster 1 includes all winter samples collected at the two sites in Shenyang. All summer samples collected at the two sites in Shenyang and summer and winter samples in Tokyo were grouped into Cluster 2. This result indicates that the compositions of PAHs and NPAHs in winter were different from the compositions in summer at the two sites in Shenyang and that the compositions of PAHs and NPAHs in summer at these sites were similar to those in Tokyo in both summer and winter. Previously, we reported that the main sources of atmospheric PAHs and NPAHs were motor vehicles in all seasons in Tokyo, while they were coal combustion systems in winter and motor vehicles and coal combustion systems in summer in Shenyang (Tang et al., 2005; Hattori et al., 2007). These results suggest that the major contributors of atmospheric PAHs and NPAHs in Shenyang did not change significantly during 2001–2002 to 2007. However, the data in Cluster 1 in Figure 3 indicate that the compositions of PAHs and NPAHs in winter at the two sites in Shenyang slightly differed between 2002 and 2007. Possible causes of the differences in 2007 include the air pollution countermeasures and the increase in the number of vehicles.

The [1-NP]/[Pyr] ratio is a useful indicator for estimating the contributions of motor vehicles and coal combustion systems to atmospheric PAHs and NPAHs (Tang et al., 2005). Although 1-NP can form during the sampling and a part of Pyr is distributed in the gas phase, the yields of 1-NP that formed in the filter were smaller than 5% and the partition ratios in the gas and particulate phases of Pyr depend on temperature (Nielsen, 1983; Yamasaki et al., 1982). Figure 4 shows the [1-NP]/[Pyr]

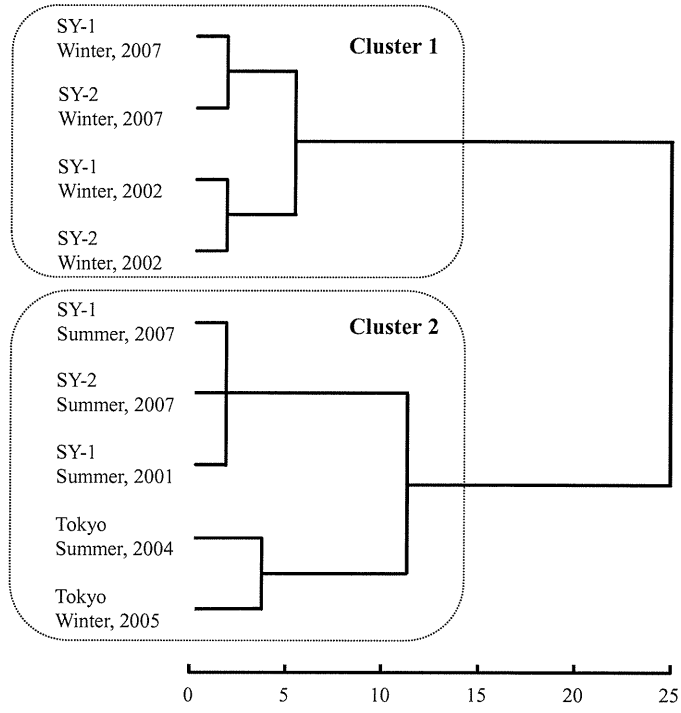

Figure 3. Cluster analysis dendrogram of atmospheric polycyclic aromatic hydrocarbons (PAHs) and nitropolycyclic aromatic hydrocarbons (NPAHs)at two sites in Shenyang and in Tokyo by using Ward's method and standardized squared Euclidean distance. The parameters used for the cluster analysis were the concentration ratios of 1-NP to Pyr, 6-NBaP to BaP and individual PAH to total PAHs in the airborne particulates collected at two sites in 2001–2002 and 2007.

ratios in the atmospheric particulates collected at the two sites of Shenyang in 2001–2002 and 2007. During the intervening 5 years, the [1-NP]/[Pyr] ratios in winter increased from 0.003 to 0.014 at SY-1 and from 0.002 to 0.010 at SY-2. In summer, the [1-NP]/[Pyr] ratios also increased from 0.008 (2001) to 0.025 (2007) at SY-1. Although no data was obtained at SY-2 in

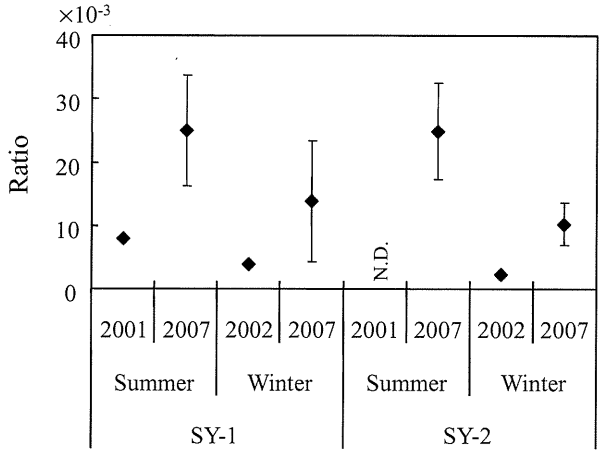

Figure 4. Graph for comparison of [1-NP]/[Pyr] ratios at two sites in Shenyang. The data of Shenyang in 2001–2002 are from Hattori et al. (2007).

summer 2001, the [1-NP]/[Pyr] ratio was very high (0.025) as well. Furthermore, the [1-NP]/[Pyr] ratio variance at SY-1 was larger in summer than in winter. The [1-NP]/[Pyr] ratio of particulates emitted by coal combustion systems (0.001) was much smaller than the ratio of particulates emitted by diesel-engine automobiles (0.36) (Tang et al., 2005). These results suggest that motor vehicles became one of the major contributors of atmospheric PAHs and NPAHs in Shenyang in 2007 not only in summer but also in winter.

Conclusions

The concentrations and distribution of PAHs and NPAHs in different particulate size fractions changed between 2001–2002 and 2007. In winter, the concentrations of coarse size particulates (>2.1 μm) in the atmosphere decreased from 57.5% to 44.6% over the 5-year period. Concurrently, the concentrations of atmospheric PAHs and NPAHs in winter in the coarse size particulate fractions, which might have originated from inefficient boilers, decreased from 0.35 pmol μg^{-1} to 0.15 pmol μg^{-1}, and 0.55 fmol μg^{-1} to 0.32 fmol μg^{-1}, respectively, during the 5 years. Especially, the concentrations of PAHs and NPAHs in winter 2007 decreased significantly from the concentrations in winter 2002, probably largely as a result of Shenyang's Blue Sky Project. However, both PAH and NPAH concentrations in summer increased from 2001 to 2007, and the concentrations of NPAHs in winter did not change markedly between 2002 and 2007. Our comparative data on the particulate distributions, seasonal variations and compositions of PAHs and NPAHs in the atmosphere show that motor vehicles have become one of the major contributors of atmospheric PAHs and NPAHs in Shenyang not only in summer but also in winter.

Acknowledgement

This research was supported in part by a Grant in Aid for Scientific Research (Nos. 21256001, 21120503 and 21590132) from the Ministry of Education, Culture, Sports, Science and Technology, Japan and Steel Industry Foundation for the Advancement of Environmental Protection Technology. This research was also a Joint Project supported by Japan-China Medical Association. The authors thank Susumu Hayakari of Aomori Prefectural Institute of Public Health and Environment, Japan for providing statistical analysis software program.

References

Arey, J., Zielinska, B., Atkinson, R., Winer, A. M., Ramdahl, T. and Pitts, J. N. 1986. The formation of nitro-PAH from the gas–phase reactions of fluoranthene and pyrene with the OH radical in the presence of NOx. *Atmospheric Environment* 20:2339–2345.

Bourotte, C., Forti, M. C., Taniguchi, S., et al. 2005. A wintertime study of PAHs in fine and coarse aerosols in Sao Paulo City, Brazil. *Atmospheric Environment* 39:3799–3811.

Hayakawa, K., Kitamura, R., Butoh, M., et al. 1991. Determination of diamino- and aminopyrenes by high performance liquid chromatography with chemiluminescence detection. *Analytical Sciences* 7:573–577.

Hayakawa, K., Murahashi, T., Butoh, M. and Miyazaki, M. 1995a. Determination of 1,3-, 1,6-, and 1,8-dinitropyrenes and 1-nitropyrene in urban air by high-performance liquid chromatography using chemiluminescence detection. *Environmental Science and Technology* 29:928–932.

Hayakawa, K., Kawaguchi, Y., Murahashi, T. and Miyazaki, M. 1995b. Distributions of nitropyrenes and mutagenicity in airborne particulates collected with an Andersen sampler. *Mutation Research* 348:57–61.

Hayakawa, K., Murahashi, T., Akutsu, K., Kanda, T., Tang, N., Kakimoto, H., Toriba, A. and Kizu, R. 2000. Comparison of polycyclic aromatic hydrocarbons and nitropolycyclic aromatic hydrocarbons in airborne and automobile exhaust particulates. *Polycyclic Aromatic Compounds* 20;179–190.

Hayakawa, K., Tang, N., Akutsu, K., et al. 2002. Comparison of polycyclic aromatic hydrocarbons and nitropolycyclic aromatic hydrocarbons in airborne particulates collected in downtown and suburban Kanazawa, Japan. *Atmospheric Environment* 36:5535–5541.

Hayakawa, K., Tang, N., Kameda, T. and Toriba, A. 2007. Atmospheric behaviors of polycyclic aromatic hydrocarbons and nitropolycyclic aromatic hydrocarbons in East Asia. *Asian Journal of Atmospheric Environment* 1:19–27.

Hattori, T., Tang, N., Tamura, K., et al. 2007. Profiles of particulate-bound polycyclic aromatic hydrocarbons and their nitrated derivatives in three typical cities, Liaoning Province, China. *Environmental Forensics* 8:165–172.

Ho, K. F., Cao, J. J., Lee, S. C. and Chan, C. K. 2006. Source apportionment of PM2.5 in urban area of Hong Kong. *Journal of Hazardous Materials* 138:73–85.

International Agency for Research on Cancer (IARC). 2005. *IARC Monographs on the Evaluation of the Carcinogenic Risks to Humans* 92.

Kakimoto, H., Kitamura, M., Matsumoto Y., et al. 2000. Comparison of atmospheric polycyclic aromatic hydrocarbons and nitropolycyclic aromatic hydrocarbons in Kanazawa, Sapporo and Tokyo. *Journal of Health Science* 46:5–15.

Kakimoto, H., Matsumoto, Y., Sakai, S., et al. 2002. Comparison of atmospheric polycyclic aromatic hydrocarbons and nitropolycyclic aromatic hydrocarbons in an industrialized city (Kitakyushu) and two commercial cities (Sapporo and Tokyo). *Journal of Health Science* 48:370–375.

Kawanaka, Y., Matsumoto, E., Sakamoto, K., et al. 2004. Size distributions of mutagenic compounds and mutagenicity in atmospheric particulate matter collected with a low–pressure cascade impactor. *Atmospheric Environment* 38:2125–2132.

Kizu, R., Ishii, K., Kobayashi, J., et al. 2000. Antiandrogenic effect of crude extract of C–heavy oil. *Materials Science and Engineering* C 12:97–102.

Kong, S., Ding, X., Bai, Z., et al. 2010. A seasonal study of polycyclic aromatic hydrocarbons in PM2.5 and PM2.5-10 in five typical cities of Liaoning Province, China. *Journal of Hazardous Materials* 183:70–80.

National Climatic Data Center. 2009, August 24. *NNDC climate data online*. Available at: http://lwf.ncdc.noaa.gov/oa/climate/online prod/drought/xmgr.html#gr

Nielsen, T. A. 1983. The formation and presence for nitro derivatives of polycyclic aromatic hydrocarbons in the atmosphere. *Proceedings of the World Congress on Air Quality* 1:239–243.

Rogge, W. F., Hildemann, L. M., Mazurek, M. A., et al. 1993. Sources of fine organic aerosol. 2. Noncatalyst and catalyst-equipped automobiles and heavy–duty diesel trucks. *Environmental Science and Technology* 27;636–651.

Shenyang Environmental Protection Bureau of China. Annual statistical report on environment in Shenyang from 2007 to 2010. http://www.syepb.gov.cn/

Tang, N., Tabata, M., Mishukov, V. F., et al. 2002a. Comparison of atmospheric nitropolycyclic aromatic hydrocarbons in Vladivostok, Kanazawa and Toyama. *Journal of Health Science* 48:30–35.

Tang, N., Oguri, M., Watanabe, Y., et al. 2002b. Comparison of atmospheric polycyclic aromatic hydrocarbons in Vladivostok, Toyama and Kanazawa. *Bulletin of the Japan Sea Research Institute, Kanazawa University* 33:77–86.

Tang, N., Toriba, A., Kizu, R., and Hayakawa, K. 2003. Improvement of an automatic HPLC system for nitropolycyclic aromatic hydrocarbons: Removal of an interfering peak and increase in the number of analytes. *Analytical Sciences* 19;249–253.

Tang, N., Hattori, T., Taga, R., et al. 2005. Polycyclic aromatic hydrocarbons and nitropolycyclic aromatic hydrocarbons in urban air particulates and their relationship to emission sources in the Pan–Japan Sea countries. *Atmospheric Environment* 39:5817–5826.

Tang, N., Araki, Y., Tamura, K., et al. 2009. Distribution and source of atmospheric polycyclic aromatic hydrocarbons and nitropolycyclic aromatic hydrocarbons in Tieling city, Liaoning Province, a typical local city in China. *Asian Journal of Atmospheric Environment* 3: 52–58.

Yamasaki, H., Kuwata, K., Miyamoto, H. 1982. Effect of ambient temperature on aspects of airborne polycyclic aromatic hydrocarbons. *Environmental Science and Technology* 16:189–194.

シリーズ　新しい内分泌現象

メラトニンの新規作用：骨に対する作用とその誘導体を用いた骨疾患治療薬の開発

鈴木　信雄[1]、関　あずさ[2]、染井　正徳[1]、中村　正久[3]、矢野　幸子[4]
大森　克徳[4]、池亀　美華[5]、三島　弘幸[6]、早川　和一[7]、服部　淳彦[8]
([1]金沢大学・環日本海域環境研究センター、[2]ハムリー株式会社・国際事業部、[3]早稲田大学・教育総合科学学術院、[4]宇宙航空研究開発機構、[5]岡山大学大学院・医歯薬学総合研究科、[6]高知学院短期大学、[7]金沢大学・医薬保健研究域、[8]東京医科歯科大学・教養部)
E-mail: nobuos@staff.kanazawa-u.ac.jp

1．はじめに

メラトニンは概日リズムを調節するホルモンであるが、骨に作用することが最近わかってきた。さらに筆者らのグループは、新規メラトニンの誘導体が骨芽細胞の活性を上昇させ、破骨細胞の活性を抑制することを魚のウロコを用いた*in vitro*評価系を用いて発見した。新規メラトニン誘導体の作用は、骨疾患モデル動物においても認められているので、骨疾患の治療薬として有望である。本稿では、メラトニンの骨に対する作用について述べ、次に新規メラトニン誘導体を用いた骨疾患の治療薬の開発について述べる。

2．メラトニンの生理作用

2-1．メラトニンの分布

メラトニンは、必須アミノ酸の1つであるトリプトファンからセロトニンを経て合成される分子量232のアミン(N-アセチル-5-メトキシトリプタミン：N-acetyl-5-methoxy-tryptamine)である。これまで一般的にメラトニンは、松果体に特異的なホルモンといわれてきた。しかし、近年、網膜や脳(大脳皮質、縫線核、線条体など)、脊髄、消化管(小腸、胃など)、精巣、卵巣、水晶体、蝸牛、皮膚、骨髄、リンパ球においても産生されることが明らかにされた[1)]。骨髄でメラトニンが産生することからも、メラトニンが骨に作用することを示唆しており、最近、メラトニンの骨代謝に対する作用を調べた研究が少しずつではあるが増えつつある。

2-2．松果体除去により引き起こされる脊柱変形

最初に骨形成に関する松果体の役割を指摘したのは、1959年のThillardの研究[2)]である。孵化直後のニワトリの松果体を除去すると、約6割から7割の個体に脊柱側彎変形が生じる。筆者の一人である服部が、実際にニワトリの松果体を除去すると、図1のように脊柱側彎変形を引き起こす。しかし、Thillardの報告ではメラトニンとの関係を直接証明したわけではなかった。さらにこの報告はフランス語で書かれていることもあり、その後、しばらく追試されることはなかった。

メラトニンの関与について調べた研究は、町田ら(1995年)[3)]により実施された。即ち、松果体を除去したニワトリに体重100 g当たり25 mgのメラトニンを隔日3週間腹腔内に投与すると、側彎発生率を20%にまで抑制できることが報告された。加藤と服部(1995年)[4)]も、松果体を除去したニワトリにメラトニン入りチューブを皮下に移植し、正常個体の夜間のメラトニンレベルに相当する濃度

図1　松果体除去ニワトリに多発する脊柱側彎変形

を維持するという方法を用いて、側彎発生率を約45％にまで抑制できることを見出した。さらに、椎骨や長管骨には、脳に存在するメラトニンレセプターと同様の生化学的特徴を持つレセプターが存在することを明らかにした[4]。しかし、その後の様々な研究にもかかわらず、現在でも、松果体を除去すると脊柱変形が生じるのかは不明のままである。メラトニンと骨代謝との研究のきっかけとなったが、メラトニンの間接的な影響である可能性や松果体にメラトニン以外の生理活性物質が存在していることも考えられ、不明な点が多い現象である。

2-3. メラトニンの骨芽細胞（*in vitro*）に対する作用

メラトニンの骨芽細胞に対する直接作用を最初に報告したのは、1999年のRothら[5]と中出ら[6]のグループである。前者は、マウスの骨芽前駆細胞株やラットの骨芽細胞様骨髄腫細胞株を用いて、骨芽細胞への分化が促進されることを示した。後者は、ヒトの骨芽細胞様細胞株を用いて、50 μMのメラトニンが約2倍の増殖を引き起こすことを報告している。しかしこれらの研究では、破骨細胞との共存培養ではなく、さらにメラトニンの濃度も高くないと効果がない。後述のウロコを用いて得られた結果の方が、破骨細胞との共存培養であり、マウスやラット等の哺乳類を用いた*in vivo*のデータに近い。

2-4. メラトニンの骨疾患モデル動物（*in vivo*）に対する作用

一般に骨粗鬆症は、原発性骨粗鬆症と続発性骨粗鬆症とに分けられる。前者の骨粗鬆症は、閉経に伴うエストロゲンの急激な分泌低下が主因となっており、高齢化に伴い社会的な問題になっている。骨は海綿骨と皮質骨より構成されているが、エストロゲンの低下により初期に海綿骨が、その後皮質骨も影響を受ける。閉経後骨粗鬆症の骨代謝は高回転型であり、骨密度減少の速度は急激であり、海綿骨の骨量減少は年間4〜8％にも及ぶ。この閉経後骨粗鬆症のモデルとして一般的に用いられるのが、人為的に卵巣を摘出したラットである。

卵巣を摘出した群では骨吸収マーカーの一つである尿中デオキシピリジノリン値が51％上昇するのに対して、メラトニン（25 μg/ml）を飲み水に溶解させて経口投与した群では、骨吸収が抑制され、卵巣摘出前と比べて変化しなかったという報告がある[7]。しかし彼らの実験では、骨組織（骨密度、骨量や骨面積）には、メラトニン投与群との間で大差は認められなかった。さらに、卵巣摘出ラットにエスラジオールを投与するとともに、メラトニンを追加投与することにより、各骨代謝マーカーの変化を調べた報告もある[8]。各マーカーに対する効果の現れ方には多少の違いはあったが、卵巣を摘出することにより上昇する骨吸収マーカーをエストラジオールは

抑制して、その効果をメラトニンがさらに補強するという報告である。

一方、正常な実験動物を用いた研究もある。即ち、4週齢の若いマウスを使った実験では、1ヶ月間かなり高濃度のメラトニン(5 mgあるいは50 mg/100 g体重)を与え続けると、骨密度が36%、骨量が49%上昇した。これらのメラトニン投与個体では骨形成パラメーターはほとんど変化しなかったが、骨吸収パラメーターは顕著に減少していた[9]。

したがって、*in vitro*の骨芽細胞の単独培養による結果とは矛盾して、*in vivo*においてメラトニンは、骨形成に作用するというよりも、骨吸収を抑制するように作用するという見解が有力である。

3．メラトニンの破骨細胞及び骨芽細胞に対する作用：キンギョのウロコを用いた*in vitro*評価系による解析

3-1．魚類のウロコの構造

硬骨魚のウロコは、石灰化した骨基質の上に骨芽細胞と破骨細胞が共存した構造をしており(図2)[10]、その基質は、I型コラーゲンからなる線維層とI型コラーゲンとハイドロキシアパタイトからなる骨質層の二層からなる。骨質層は骨芽細胞によって膜内骨化と同様の様式で形成される。また、ウロコに存在する破骨細胞は多くは単核であるが、多核で波状縁を持つものも観察され、そのような破骨細胞は哺乳類の破骨細胞と同様の微細構造をもち(図3)[11]、カテプシンKや酒石酸抵抗性酸フォスファターゼが発現している(図4)[12]。

3-2．魚類のウロコを用いた評価システムの開発と様々な物質に対する応答

筆者らはこのような特徴を持つウロコを培養し、生理学的活性を指標とした評価システムを開発した。ウロコの培養には炭酸ガスは不要であり、培地には血清不含のL-15(水生動物用の培地)に抗生物質を入れて用い、低温(15℃)で少なくとも1週間培養可能である。

このシステムを用いて、骨代謝に関与するホルモン等の作用を調べると、以下のことが判明した。カルシトニンが哺乳類と同様にウロコの破骨細胞の活性を抑制することを証明した[13]。カルシトニン(100 ng/ml)のウロコの破骨細胞に対する作用は、淡水産のキンギョでも海産魚のメジナでもみられ、淡水産のキンギョの方がその効果が強かった。さらにキンギョでは、雌雄共にカルシトニンの効果が認められたが、メジナでは雌のみしか効果がなかった。そこで入手・飼育も容易なキンギョを主な実験材料として用いて、これまで実験をしている。

副甲状腺ホルモン、エストロゲン、インスリン様成長因子I及び活性型ビタミンD_3の骨芽細胞に対する作用も解析済みであり、カルシトニン、副甲状腺ホルモン、エストロゲン及び活性型ビタミンD_3の受容体もウロコからクローニングしている[11, 14〜16]。

さらにウロコのシステムの感度は良く、極めて低濃度(10^{-13}M)のカドミウムにも応答

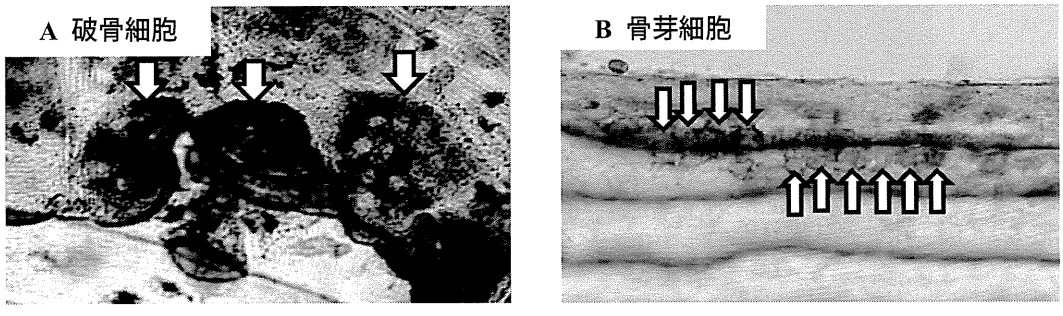

図2　キンギョのウロコに存在する破骨細胞(A)と骨芽細胞(B)(文献10より改変)
A：酒石酸抵抗性酸フォスファターゼの活性染色
B：アルカリフォスファターゼの活性染色
図中の矢印は、破骨細胞及び骨芽細胞を示す。

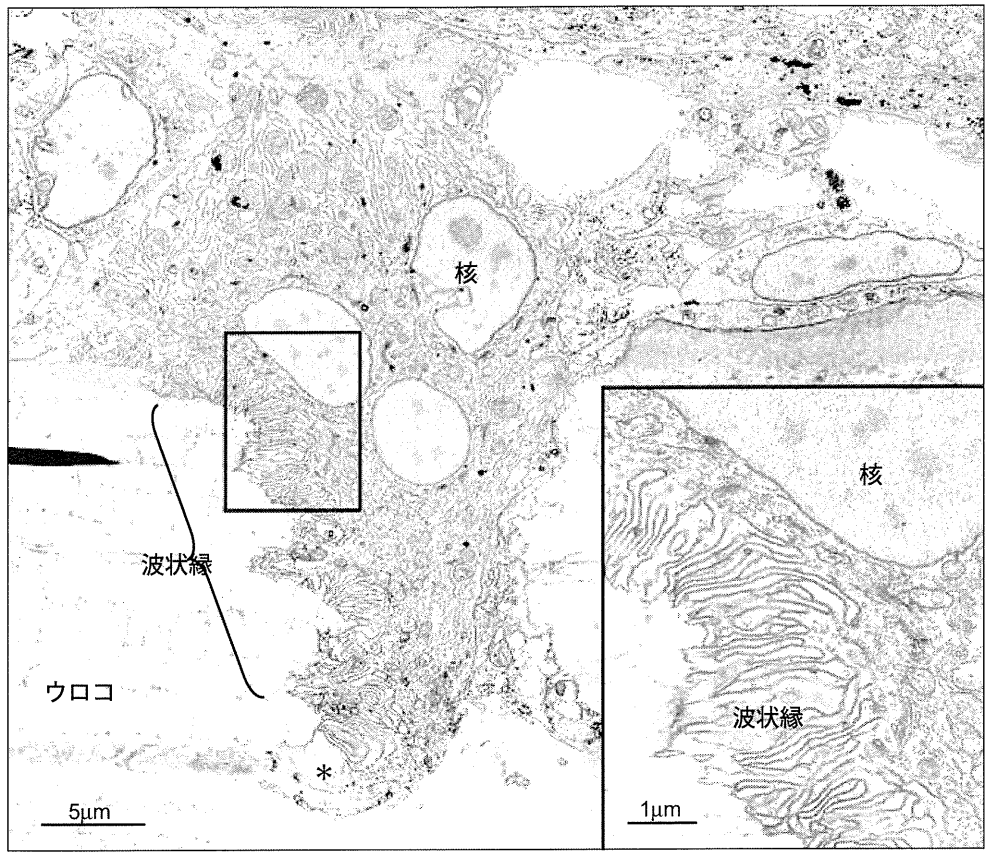

図3　副甲状腺ホルモン処理により活性化した破骨細胞の電子顕微鏡写真（文献11より改変）

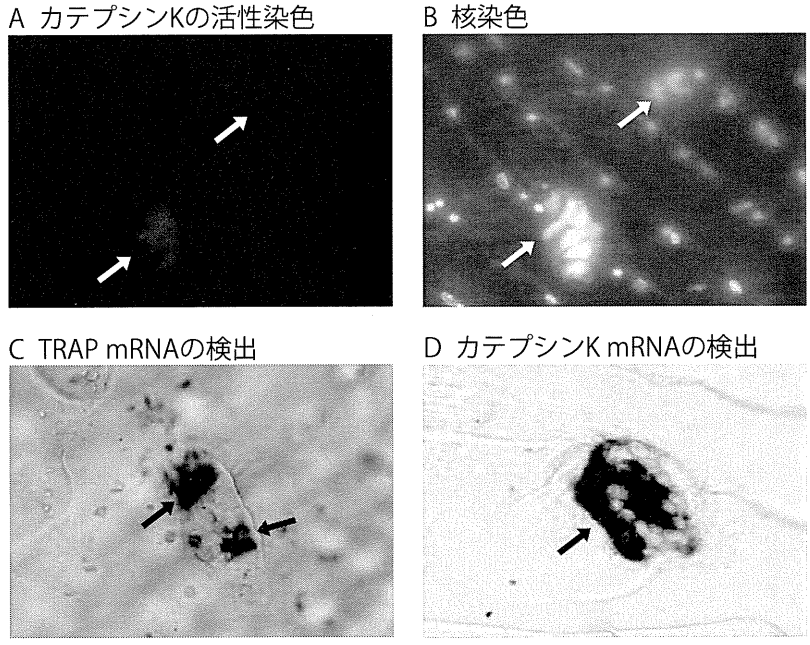

図4　キンギョのウロコに存在する破骨細胞（文献12より改変）

A：カテプシンKの活性染色
B：4',6-diamino-2-phenylindoleを用いた核染色
C：*in situ*ハイブリダイゼーション法による酒石酸抵抗性酸フォスファターゼ（TRAP）mRNAの検出
D：*in situ*ハイブリダイゼーション法によるカテプシンK mRNAの検出
図中の矢印は、破骨細胞を示す。

し[17]、内分泌攪乱化学物質であるトリブチルスズ[18]や重油に含まれる成分である多環芳香族炭化水素に対しても鋭敏に反応する[19]。

3-3. 破骨細胞及び骨芽細胞で特異的に発現しているマーカー遺伝子のクローニング

最近哺乳類において、骨芽細胞と破骨細胞の相互作用に関係する遺伝子が明らかにされた[20]。この遺伝子は骨芽細胞で特異的に発現しているReceptor Activator of NF-κB Ligand (RANKL) と破骨細胞で発現しているReceptor Activator of NF-κB (RANK) である。特に、破骨細胞を多核の活性型に誘導するには、骨芽細胞との連絡が必要であり、RANKLがリガンドとなり、破骨細胞のレセプターであるRANKと結合しなければ多核の活性型に誘導されない。これらの遺伝子は、哺乳類でしかクローニングされていなかったが、最近キンギョのウロコからcDNAの全長のクローニングに成功した。この遺伝子の発現を解析することで、骨芽細胞と破骨細胞とのクロストークを解析できる。そこで副甲状腺ホルモンの作用を解析した結果、骨芽細胞の活性は6時間培養で上昇し、培養18時間後に破骨細胞の活性が上昇するという結果が得られた[11]。その活性の変化の理由としてRANK 及びRANKLの関与を証明した。すなわち、RANK mRNAの発現が顕著に上昇し、破骨細胞の活性が上昇することを証明した[11]。

さらに前述の破骨細胞のマーカー(カテプシンKや酒石酸抵抗性酸フォスファターゼなど)に加えて、骨芽細胞で発現しているI型コラーゲン、オステオカルシン、アルカリフォスファターゼ、オステリックス、Runx 2 (runt-related transcription factor 2) も既にクローニング済みであり、これらについても解析可能である。したがって、ウロコの評価システムは骨のモデルとして遺伝子レベルからアプローチすることができる。

3-4. メラトニンの破骨細胞及び骨芽細胞に対する作用

ウロコの評価システムを用いて、メラトニンの破骨細胞と骨芽細胞に対する作用を解析した。その結果、メラトニンが、破骨細胞や骨芽細胞に対して抑制的に作用することを、脊椎動物を通して初めて明らかにした[21]。これらのメラトニンの作用は、骨芽細胞で発現しているインスリン様成長因子-I mRNAやエストロゲン受容体mRNAの発現を低下させることによって引き起こされていた。なお、ウロコにメラトニン受容体が発現していることも確認している[22]。

前述のように骨芽細胞の単独培養では、薬理的な量のメラトニンは骨芽細胞の増殖促進に作用するが、ラットを用いた*in vivo*の実験では、メラトニンを投与すると、血液中のALP活性が低下することが報告されており[8]、筆者らのウロコの評価系の方が*in vivo*の状態を再現していることを示している。

4．骨疾患の治療薬としての新規メラトニン誘導体

4-1. 新規メラトニン誘導体のウロコの骨芽細胞及び破骨細胞に対する応答

メラトニンの骨に対する作用が明確になったので、新規メラトニン誘導体を合成して骨芽細胞及び破骨細胞に対する作用をメラトニンと比較した[23]。即ち、メラトニン、2-ブロモメラトニン、2,4,6-トリブロモメラトニン、1-アリル-2,4,6-トリブロモメラトニン、1-プロパルギル-2,4,6-トリブロモ-メラトニン、1-ベンジル-2,4,6-トリブロモメラトニン及び2,4,6,7-テトラブロモメラトニン(図5)を合成して、これら化合物の破骨細胞及び骨芽細胞に対する作用をキンギョのウロコを用いた培養系で評価した。培養時間は6時間で、濃度は10^{-8}、10^{-6}、10^{-4} Mでその作用を解析した。培養方法等の詳細は、鈴木と服部(2002)[21]の方法に従った。

次に最も効果があった化合物において、6時間及び18時間培養で、10^{-10}、10^{-9}、10^{-8}、

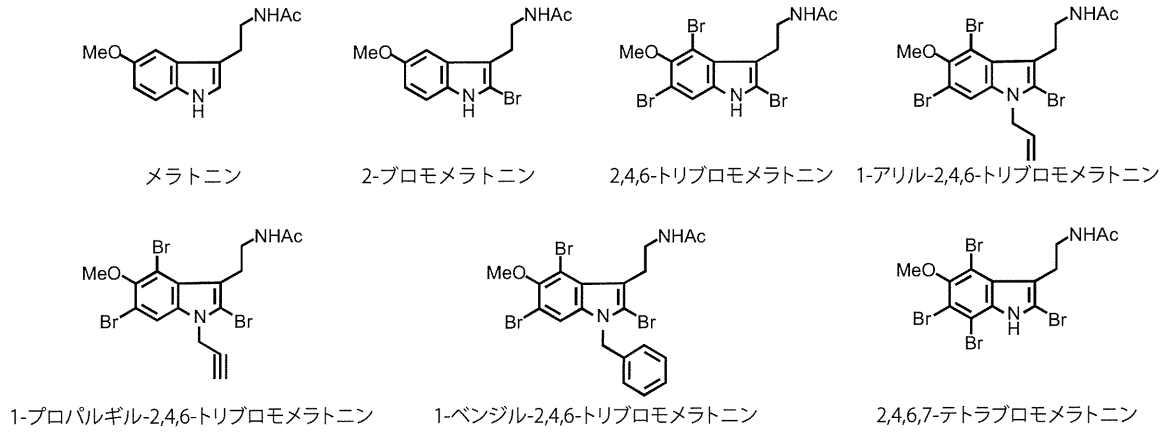

図5　メラトニンと新規メラトニン誘導体の構造式（文献10より改変）

10^{-7}及び10^{-6}Mにおいて、骨に対する作用をメラトニンと比較した。さらに、骨芽細胞で発現しているエストロゲン受容体mRNAの発現（6時間培養）に対する影響も解析した。

その結果、メラトニンは骨芽細胞の活性を低下させたが、Br原子を導入した全ての誘導体は、骨芽細胞の活性を上昇させることが判明した。一方、Br原子を3個導入した誘導体では破骨細胞の活性抑制作用は強く、メラトニンと同程度であった。しかしBr原子を1及び4個入れた誘導体では、メラトニンの方が破骨細胞の活性抑制作用は強かった。今回調べた化合物の中で、特に1-ベンジル-2,4,6-トリブロモメラトニンの骨芽細胞の活性を上昇させる作用は強く、この化合物を用いてさらに詳細に調べた。

結果を図6及び7に示す。1-ベンジル-2,4,6-トリブロモメラトニンはメラトニンと異なり、骨芽細胞の活性を上げ、その作用は18時間後でも持続しており、10^{-8} Mでも効果が認められた。また1-ベンジル-2,4,6-トリブロモメラトニンの破骨細胞の活性抑制作用は、メラトニンのそれよりも強く、6時間培養で10^{-10} Mでも効果が認められた。さらに骨芽細胞のマーカーであるエストロゲン受容体 mRNAの発現は、1-ベンジル-2,4,6-トリ

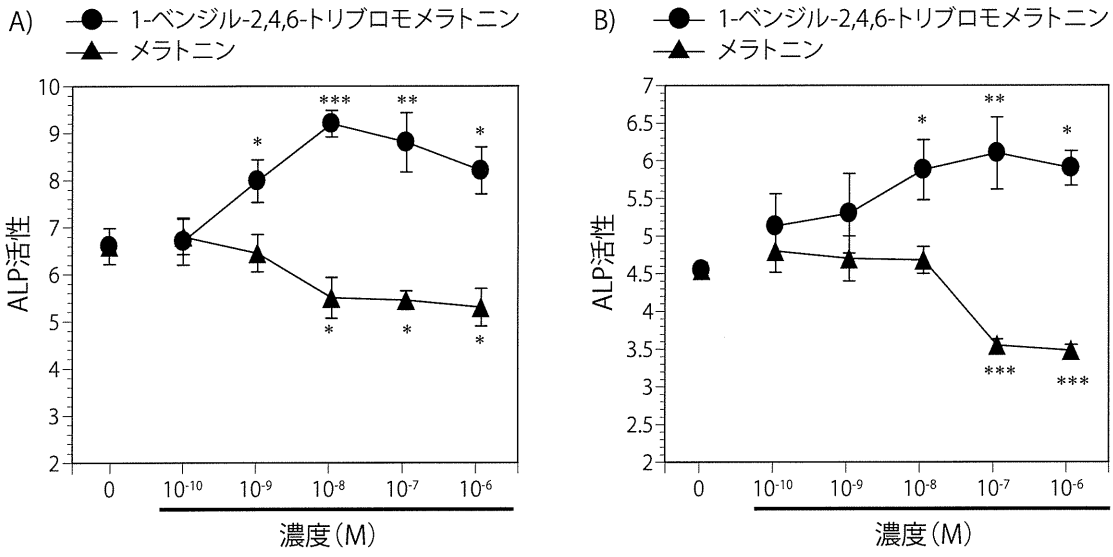

図6　新規メラトニン誘導体のキンギョのウロコの骨芽細胞に対する作用（文献23より改変）
A：6時間培養の結果　　B：18時間培養の結果
*：P＜0.05；**：P＜0.001；***：P＜0.001

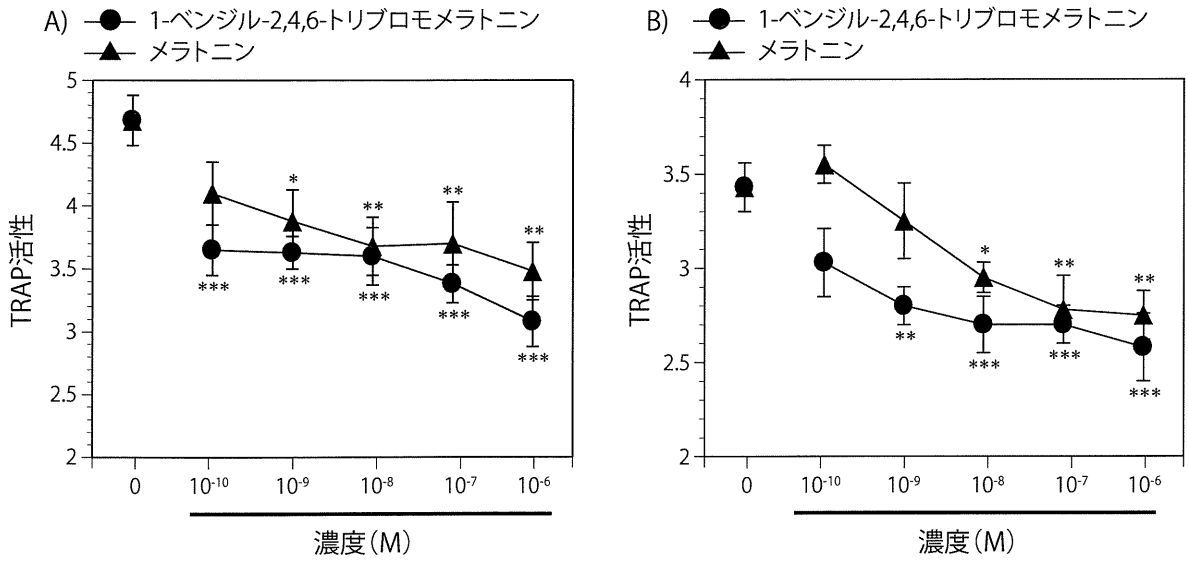

図7　新規メラトニン誘導体のキンギョのウロコの破骨細胞に対する作用（文献23より改変）
A：6時間培養の結果　　B：18時間培養の結果
*：P＜0.05；**：P＜0.001；***：P＜0.001

ブロモメラトニン処理で有意に上昇することも判明した。

4-2. 新規メラトニン誘導体の変異原性試験及び急性毒性試験

新規メラトニン誘導体を用いた骨疾患治療薬の開発の基礎として変異原性試験（エームス試験）と急性毒性試験を行った。

エームス試験は、大腸菌とサルモネラ菌を用いて、プレート（25 ml）当たり、新規メラトニン誘導体（1-ベンジル-2,4,6-トリブロモメラトニン）を8、40、200、1,000、3,000及び5,000 μg添加して、コロニー数をカウントした。その結果、化合物の添加量が変化してもコロニーの数は変化せず、ジメチルスルホキシドを添加したコントロールとほとんど同じコロニー数だった。したがって、この化合物の変異原性は認められなかった。

次にラットに新規メラトニン誘導体を2,000 mg/kgの割合で単回経口投与して、14日間観察して、急性毒性を調べた。その結果、ラットの行動及び食欲にも変化はみられず、死亡する個体もみられなかった。さらに、解剖して肝臓等の主要臓器を検査した結果、異常は認められなかった。

以上のことから、新規メラトニン誘導体には変異原性も急性毒性もみられないことが明らかになった。

4-3. 骨疾患モデル動物に対する作用

これまで骨粗鬆症の治療薬は骨吸収を抑制する薬剤（ビスフォスフォネイト）が主流であり、骨吸収を抑制してかつ骨形成を顕著に促進する薬剤は未だ開発されていない。そこで、卵巣摘出ラットを用いて新規メラトニン誘導体の実験を行った。その結果、卵巣摘出ラットの大腿骨の海綿骨の骨密度が上がり、骨強度が有意に上昇した（図8）。

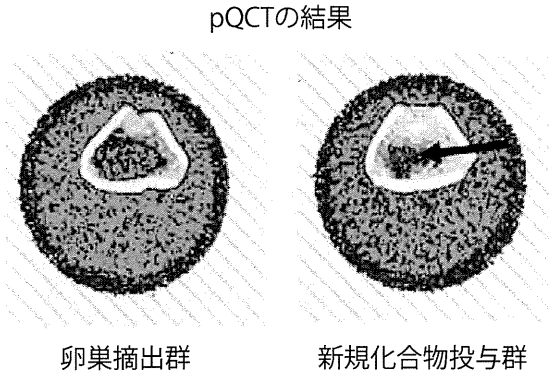

図8　新規メラトニン誘導体の卵巣摘出ラットに対する作用
矢印は、骨形成が促進された部分を示す。

さらにカルシウムの摂取量が少ない現代人の食生活から引き起こされる骨疾患モデル(低カルシウム食ラット)でも、大腿骨の海綿骨の骨密度が有意に上昇した[10]。メラトニンは、骨吸収を抑制したが、新規メラトニン誘導体は骨吸収抑制に加えて骨形成も促進している可能性がある。現在、大腿骨を外科的に切断したラット(骨折モデル動物)を用いて実験中であり、骨形成を促進する治療薬になる可能性を秘めている。

4-4. 新規メラトニン誘導体を用いた宇宙実験

骨のモデルとして魚類(キンギョ)のウロコを使用して「きぼう」の国際宇宙ステーションを用いた宇宙実験を2010年5月に実施した。本実験の目的は、①宇宙における骨量減少のしくみを探ること、②骨形成を促す物質(新規メラトニン誘導体)の効果を調べること、である。

前述のようにウロコには骨芽細胞と破骨細胞が共存していること(図2)に注目して、ウロコの培養システムを開発した。骨量維持には、骨の形成系(骨芽細胞)と骨の吸収系(破骨細胞)のバランスが保たれていなければならない。骨芽細胞は、重力の刺激をうけると活性化することが知られている。しかし宇宙空間では、重力の刺激がないため、骨量が減少する。そこで、①メカニズムを解明して、②骨量減少を抑制する薬剤の効果を調べた。

宇宙実験の概要[24]を図9に示す。筆者らが提案した宇宙実験は、野口総一宇宙飛行士により実施された。現時点での解析結果から新規メラトニン誘導体の効果は確認できており、前述の骨疾患モデル動物の結果と合わせて考えると、本物質は骨疾患治療薬として有望である。

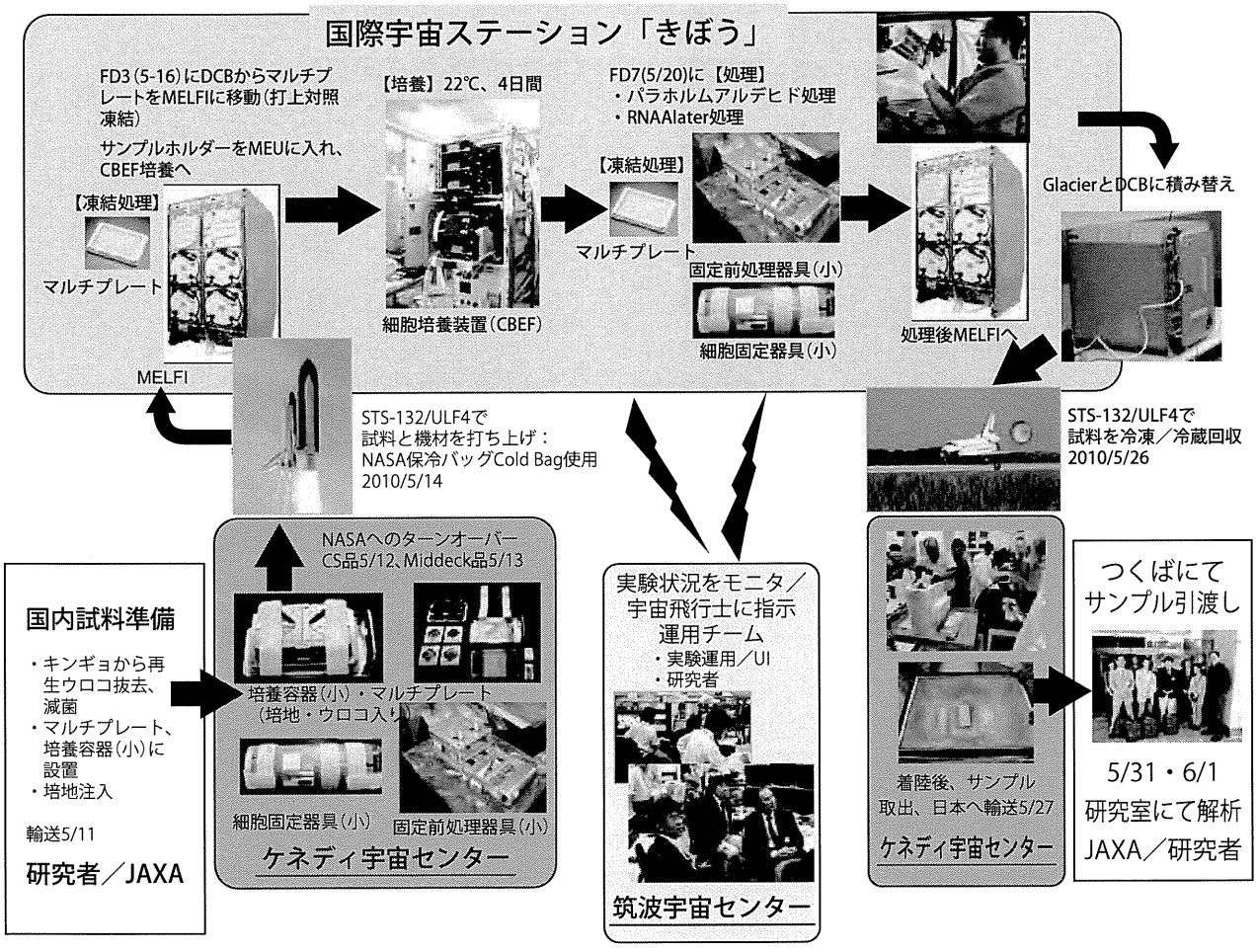

図9　宇宙実験の概要(文献24より改変)

5．おわりに

本稿では、メラトニン及びその誘導体の硬組織(骨とウロコ)に対する作用に注目した。しかしメラトニンは、植物にも含まれており、現時点では、植物においては、受容体を介した作用ではなく、ラジカル除去に作用している可能性が高い[1)]。メラトニン自身のラジカル消去作用にとどまらず、メラトニンから酵素的、酸化的に生成したN^1-acetyl-N^2-formyl-5-methoxykynuramine(N^1-アセチル-N^2-ホルミル-5-メトキシキヌラミン)などが、ラジカルを除去すると考えられている[25)]。メラトニンは元来、ヒトの体内で作られるホルモンなので、過剰摂取しても副作用がない。今後、骨に対する作用以外にも、ラジカル除去作用のあるメラトニンは、「抗加齢薬」として広まる時期が来る可能性がある。

謝　辞

本研究の一部は、科学研究費補助金、クリタ水・環境科学振興財団、環境省の地球環境研究総合推進費(B-905)、厚生労働科学研究費補助金、科学技術振興機構のシーズ発掘試験、宇宙航空研究開発機構の助成金により行われた。さらに、宇宙実験の実施にあたり、宇宙環境利用科学委員会研究チームのメンバー、野口総一宇宙飛行士、JAXA、JSF、JAMMSの方々の協力に感謝申し上げる。

文　献

1) 服部淳彦、2004. 自然界におけるメラトニンの分布. “メラトニン研究の最近の進歩”、星和書店、東京、p17-44.
2) Thillard MJ, 1959. Deformation de la colonne vertebrale consecutives a lepiphysectomie chez le poussin. Extrait des Comptes Rendus de I'Association des Anatomistres, **XLVI**, 22- 29.
3) Machida M, Dubousset J, Imamura Y, Iwaya T, Yamada T, Kimura J, 1995. Role of melatonin deficiency in the development of scoliosis in pinealectomised chickens. J Bone Joint Surg, **77**, 134-138.
4) Katoh H, Hattori A, 1995. Experimental scoliosis produced by pinealectomy and characterization of melatonin binding sites in vertebrae of chicks. St Marianna Med J, **23**, 853-861.
5) Roth JA, Kim B-G, Lin W-L, Cho M-I, 1999. Melatonin promotes osteoblast differentiation and bone formation. J Biol Chem, **274**, 22041-22047.
6) Nakade O, Koyama H, Ariji H, Yajima A, Kaku T, 1999. Melatonin stimulates proliferation and type I collagen synthesis in human bone cells *in vitro*. J Pineal Res, **27**, 106-110.
7) Ladizesky MG, Cutrera RA, Boggio V, Somoza J, Centrella JM, Mautalen C, Cardinali DP, 2001. Effect of melatonin on bone metabolism in ovariectomized rats. Life Sci, **70**, 557-565.
8) Ladizesky MG, Boggio V, Albornoz LE, Castrillón PO, Mautalen C, Cardinali DP, 2003. Melatonin increases oestradiol-induced bone formation in ovariectomized rats. J Pineal Res, **34**, 143-151.
9) Koyama H, Nakade O, Takada Y, Kaku T, Lau KH, 1999. Melatonin at pharmacologic doses increases bone mass by suppressing resorption through down-regulation of the RANKL-mediated osteoclast formation and activation. J Bone Miner Res, **17**, 1219-1229.
10) Suzuki N, Somei M, Seki A, Reiter RJ, Hattori A, 2008. Novel bromomelatonin derivatives as potentially effective drugs to treat bone diseases. J Pineal Res, **45**, 229-234.
11) Suzuki N, Danks JA, Maruyama Y, Ikegame M, Sasayama Y, Hattori A, Nakamura M, Tabata MJ, Yamamoto T, Furuya R, Saijoh K, Mishima H, Srivastav AK, Furusawa Y, Kondo T, Tabuchi Y, Takasaki I, Chowdhury VS, Hayakawa K, Martin TJ, 2011. Parathyroid hormone 1 (1-34) acts on the scales and involves calcium metabolism in goldfish. Bone, **48**, 1186-1193.
12) Azuma K, Kobayashi M, Nakamura M, Suzuki N, Yashima S, Iwamuro S, Ikegame M, Yamamoto T, Hattori A, 2007. Two osteoclastic markers expressed in multinucleate osteoclasts of goldfish scales. Biochem Biophys Res Commun, **362**, 594-600.
13) Suzuki N, Suzuki T, Kurokawa T, 2000. Suppression of osteoclastic activities by calcitonin in the scales of goldfish (freshwater teleost) and nibbler (seawater teleost). Peptides, **21**, 115-124.
14) Suzuki N, Hattori A, 2003. Bisphenol A suppresses osteoclastic and osteoblastic activities

in the cultured scales of goldfish. Life Sci, **73**, 2237-2247.
15) Yoshikubo H, Suzuki N, Takemura K, Hoso M, Yashima S, Iwamuro S, Takagi Y, Tabata MJ, Hattori A, 2005. Osteoblastic activity and estrogenic response in the regenerating scale of goldfish, a good model of osteogenesis. Life Sci, **76**, 2699-2709.
16) 鈴木信雄、2005. 魚類のカルシトニンの特徴. Clinical Calcium, **15**, 459-466.
17) Suzuki N, Yamamoto M, Watanabe K, Kambegawa A, Hattori A, 2004. Both mercury and cadmium directly influence calcium homeostasis resulting from the suppression of scale bone cells: The scale is a good model for the evaluation of heavy metals in bone metabolism. J Bone Miner Metab, **22**, 439-446.
18) Suzuki N, Tabata MJ, Kambegawa A, Srivastav AK, Shimada A, Takeda H, Kobayashi M, Wada S, Katsumata T, Hattori A, 2006. Tributyltin inhibits osteoblastic activity and disrupts calcium metabolism through an increase in plasma calcium and calcitonin levels in teleosts. Life Sci, **78**, 2533-2541.
19) Suzuki N, Hayakawa K, Kameda K, Toriba A, Tang N, Tabata MJ, Takada K, Wada S, Omori K, Srivastav AK, Mishima H, Hattori A, 2009. Monohydroxylated polycyclic aromatic hydrocarbons inhibit both osteoclastic and osteoblastic activities in teleost scales. Life Sci, **84**, 482-488.
20) Teitelbaum SL, 2000. Bone resorption by osteoclasts. Science, **289**, 1504-1508.
21) Suzuki N, Hattori A, 2002. Melatonin suppresses osteoclastic and osteoblastic activities in the scales of goldfish. J Pineal Res, **33**, 253-258.
22) Ikegami T, Azuma K, Nakamura M, Suzuki N, Hattori A, Ando H, 2009. Diurnal expressions of four subtypes of melatonin receptor genes in the optic tectum and retina of goldfish. Comp Biochem Physiol part A, **152**, 219-224.
23) Suzuki N, Somei M, Kitamura K, Reiter RJ, Hattori A, 2008. Novel bromomelatonin derivatives suppress osteoclastic activity and increase osteoblastic activity: Implications for the treatment of bone diseases. J Pineal Res, **44**, 326-334.
24) 鈴木信雄、北村敬一郎、清水宣明、染井正徳、笹山雄一、大森克徳、矢野幸子、重藤祐子、谷垣文章、鈴木ひろみ、嶋津徹、池亀美華、田渕圭章、高崎一朗、和田重人、近藤 隆、遠藤雅人、中村正久、井尻憲一、田畑 純、奈良雅之、服部淳彦、2011. 魚類のウロコを用いた宇宙生物学的研究、平成22年度JAROS宇宙環境利用の展望、第2章, 1-13.
25) Tan DX, Manchester LC, Burkhardt S, Sainz RM, Mayo JC, Kohen R, Shohami E, Huo YS, Hardeland R, Reiter RJ, 2001. N^1-acetyl-N^2-formyl-5-methoxykynuramine, a biogenic amine and melatonin metabolite, functions as a potent antioxidant. FASEB J, **15**, 2294-2296.

General and Comparative Endocrinology 173 (2011) 438–446

Contents lists available at ScienceDirect

General and Comparative Endocrinology

journal homepage: www.elsevier.com/locate/ygcen

Pigment-dispersing activities and cortisol-releasing activities of melanocortins and their receptors in xanthophores and head kidneys of the goldfish *Carassius auratus*

Yuki Kobayashi [a,1], Hiroaki Chiba [a], Kanta Mizusawa [a], Nobuo Suzuki [b], José Miguel Cerdá-Reverter [c], Akiyoshi Takahashi [a,*]

[a] School of Marin Biosciences, Kitasato University, 1-15-1 Kitasato, Minami-ku, Sagamihara, Kanagawa 252-0373, Japan
[b] Noto Marine Laboratory, Institute of Nature and Environmental Technology, Kanazawa University, Ogi, Noto-cho, Ishikawa 927-0553, Japan
[c] Instituto de Acuicultura de Torre de la Sal, CSIC, Torre de la Sal, Ribera de Cabanes, 12595 Castellón, Spain

ARTICLE INFO

Article history:
Received 3 March 2011
Revised 23 June 2011
Accepted 30 June 2011
Available online 19 July 2011

Keywords:
Adrenocorticotropic hormone (ACTH)
Cortisol-release
Goldfish
Melanocortin
Melanocortin receptor
Melanocyte-stimulating hormone (MSH)
Pigment-dispersion

ABSTRACT

The five subtypes of melanocortin receptors (MCRs) mediate the functions of α-melanocyte-stimulating hormone (α-MSH) and adrenocorticotropic hormone (ACTH). In fish, these hormones are involved in pigment dispersion and cortisol release, respectively. α-MSH-related peptides exhibit ACTH-like activity in certain fishes. We recently found that multiple *Mcr* transcripts are expressed in some cell types in the barfin flounder, which is related to regulation of α-MSH activities. Similar results were also observed for the cortisol-releasing activity of α-MSH-related peptides in the head kidney. The present study was undertaken to assess relationship between the expression of multiply expressed *Mcrs* and α-MSH activities using goldfish. We also determined if α-MSH-related peptides exhibit ACTH-like activity in goldfish. The transcripts of *Mc1r*, but not those of other subtypes, were observed in xanthophores. α-MSH, which has an acetyl group at the N-terminus, was found to disperse pigment in a dose-dependent manner in xanthophores. This potency was found to be slightly greater than that of desacetyl-α-MSH. These results support our findings that MCR has a higher affinity for α-MSH when single *Mcr* subtype is expressed. On the other hand, transcripts of *Mc2r*, but not those of other subtypes, were observed in the head kidney. $ACTH_{1-24}$-stimulated cortisol release was observed in a dose-dependent manner, while α-MSH-related peptides showed no activity. It therefore appears that MC2R also acts as an ACTH-specific receptor in goldfish and that association of α-MSH-related peptides upon release of cortisol is uncommon in fishes.

1. Introduction

α-Melanocyte-stimulating hormone (α-MSH) and adrenocorticotropic hormone (ACTH) are peptide hormones liberated from a common precursor known as proopiomelanocortin (POMC) [54–56]. While POMC is biosynthesized in both the pars distalis (PD) and the neurointermediate lobe (NIL) of the pituitary in teleost fish, ACTH is mainly produced in the PD, and α-MSH in the NIL in a manner that depends upon tissue-specific proteolytic cleavage [6,21,35,39,51]. While ACTH is generally composed of 39 amino acid residues, α-MSH is identical to *N*-acetyl-$ACTH_{1-13}$-amide. ACTH, α-MSH, and their related peptides are collectively classified as melanocortins (MCs) on the basis of the presence of the common amino acid sequence—His-Phe-Arg-Trp [12].

MC receptors (MCRs) are members of the G protein-coupled receptor (GPCR) family. The members of this family have seven transmembrane domains [16,33,34]. MC system consisting of POMC and MCRs in fish have been shown to be similar to that of mammals. For example, the ACTH signal is mainly mediated by the MC2 receptor (MC2R), which is one of the five subtypes of MCRs [23,48]. While MC2R selectively binds ACTH, ACTH can bind to other MCRs in addition to MC2R [1,23,48]. Although α-MSH does not bind to MC2R, the signal of α-MSH, is mediated by other MCRs. The representative biological activities of ACTH and α-MSH (including cortisol release from interrenal cells [3,57,60] and pigment dispersion [12,14,15], respectively) are related to tissue-specific expression of different MCR subtypes [33]. However, the studies on the biological activities of the MC system using barfin flounder, *Verasper moseri*, a teleost, have shown interesting relationships between different molecular forms of α-MSH-related peptides and MCRs [25–27,56].

The barfin flounder is a large commercially important flatfish that inhabits the Pacific coast of northern Japan. We demonstrated the existence of pigment-dispersing activities of α-MSH-related peptides in skin parts [26]. Interestingly, while α-MSH modified with a monoacetyl group at N-terminus was found to mediate

* Corresponding author. Fax: +81 42 778 5010.
E-mail address: akiyoshi@kitasato-u.ac.jp (A. Takahashi).
[1] Present address: Graduate School of Integrated Arts and Sciences, Hiroshima University, 1-7-1 Kagamiyama, Higashi-Hiroshima, Hiroshima 739-8521 Japan.

0016-6480/$ - see front matter © 2011 Elsevier Inc. All rights reserved.
doi:10.1016/j.ygcen.2011.06.019

dispersion of pigments in xanthophores, this peptide exhibited negligible pigment-dispersing activities in melanophores. On the contrary, desacetyl (Des-Ac)-α-MSH, which lacks the acetyl group, has pigment-dispersing activities in both xanthophores and melanophores, while the activities in xanthophores were found to be lower than the activities caused by α-MSH. Subsequently, we identified expression of only *Mc5r* in xanthophores and concomitant expression of *Mc1r* and *Mc5r* in melanophores [27]. Similar relationships between the degree of acetylation and biological activities were also observed for *in vitro* cortisol-releasing activities in the barfin flounder. While Des-Ac-α-MSH–stimulated cortisol release from interrenal cells was observed, α-MSH showed negligible effects. Moreover, both *Mc2r* and *Mc5r* were expressed in the interrenal cells [25].

There is a growing body of evidence indicating that many GPCRs form heterodimers that may affect ligand affinity [2,5,13, 28,32,36,38,43,47]. Therefore, the concomitant expression of the different *Mcr* subtypes in melanophores and interrenal cells led to the assumption that a heterodimer consisting of MC1R and MC5R in melanophores, or MC2R and MC5R in interrenal cells, may have low binding affinity for α-MSH [25,27]. This assumption conversely suggests that expression of only one *Mcr* subtype may lead to enhancement of biological activity of α-MSH relative to that of Des-Ac-α-MSH. In fact, acetylation enhances the activities of α-MSH-related peptides via MCRs expressed in human embryonic kidney-293 cells [44–46]. The present studies were undertaken to examine these possibilities using pigment cells and head kidney tissues from goldfish, *Carassius auratus*. We also determined if the cortisol-releasing activities of α-MSH-related peptides are common to goldfish by determining whether other *Mcrs*, in addition to *Mc2r*, are expressed in goldfish head kidney.

2. Materials and methods

2.1. Fish

Immature goldfish, *C. auratus*, were obtained from a commercial dealer in Shizuoka, Japan, and all experiments were conducted according to the Guidelines for the Care and Use of Animals of Kitasato University. The fish were reared in indoor tanks with circulating freshwater under a natural photoperiod. The average body sizes of the fish used for molecular cloning and gene expression tests and pigment-dispersing activities were 4.9 cm, standard length (SL), and 3.9 g body weight (BW). For these experiments, tissue samples were collected from fish anesthetized with 0.2% 2-phenoxyethanol, and subsequently frozen in dry ice/ethanol bath. Skin samples used for measurements of pigment-dispersing activities and for cell dispersion were collected from fish (4.9 cm SL, 4.1 g BW on average) anesthetized with ice-cold water. Head kidneys used in experiments for cortisol-releasing activities were collected from fish (13.5 cm SL, 87 g BW on average) anesthetized with 0.2% 2-phenoxyethanol.

2.2. Peptides

α-MSH was purchased from the Peptide Institute (Osaka, Japan). Diacetyl (Di-Ac)-α-MSH was purchased from Sigma Chemical (St. Louis, MO, USA). Des-Ac-α-MSH and $ACTH_{1-24}$ were synthesized and purified according to the previously described methods [53]. The amino acid sequence of $ACTH_{1-24}$, which is identical to that of barfin flounder ACTH-A, salmon ACTH-A, and tuna ACTH [52], differs by one residue with respect to the sequence of goldfish ACTH at position 20 (Ile in goldfish *vs* Val in others) [11].

2.3. Molecular cloning

2.3.1. Nucleic acid preparation for sequence determination

Total RNA was extracted from brain and head kidney using Isogen (Nippon Gene, Tokyo, Japan). First-strand cDNAs were synthesized from total brain RNA for amplification of *Mc1r* and *Mc3r*, cDNA, and from head kidney RNA for *Mc2r* cDNA with the SMART RACE cDNA Amplification Kit (BD Biosciences, Palo Alto, CA, USA). Custom oligonucleotides were synthesized at Nihon Gene Research Labs, Inc. (Sendai, Japan).

2.3.2. Amplification of DNA fragments for sequence determination

Polymerase chain reaction (PCR) using a thermal cycler (MJ Mini, BIO-RAD, Hercules, CA, USA) under conventional conditions was performed to amplify the DNA fragments with HotStar Taq Master Mix (Qiagen, Hilden, Germany), or Takara LA Taq (Takara, Otsu, Japan). Amplification procedures were common for all three *Mcr* cDNAs. First, the middle segment of the cDNA of each *Mcr* was amplified from first-strand cDNA by PCR using HotStar Taq DNA polymerase with primers designed from fish *Mcr* nucleotide sequences. Then, the 3′ region of each *Mcr* cDNA was amplified from first-strand cDNA by 3′ rapid amplification of cDNA ends (3′RACE) using HotStar Taq DNA polymerase with a gene-specific primers and Universal Primer A Mix (UPM) provided in the SMART RACE cDNA Amplification Kit. The 5′ region of each *Mcr* cDNA was amplified from first-strand cDNA by 5′RACE using HotStar Taq DNA polymerase with UPM and gene-specific primers. Finally, each *Mcr* cDNA containing the full-length reading frame was amplified from first-strand cDNA by PCR using HotStar Taq DNA polymerase with gene-specific primers. Primer sequences are listed in Table 1.

2.3.3. Sequence determination and data processing

PCR-amplified DNA was purified by agarose gel electrophoresis (NuSieve GTG Agarose; Cambrex Bio Science, Rockland, ME, USA). DNA was extracted from the agarose gel using a QIAEX II Gel Extraction Kit (Qiagen), ligated into plasmid pT7 Blue T-Vector (Novagen, Madison, WI, USA) or pSTBlue-1 AccepTor Vector (Novagen) and transfected into JM109-competent cells. Recombinant plasmid DNA was prepared using the alkaline-SDS method and both strands were sequenced using a capillary DNA sequencer (3130-Avant Genetic Analyzer; Applied Biosystems, Foster City, CA, USA) using the BigDye Terminator Cycle Sequencing Ready Kit ver. 3.1. DNASIS-Pro (Hitachi Software Engineering, Yokohama, Japan) was used to process nucleotide and amino acid sequences, to calculate amino acid sequence identity, to align amino acid sequences, and to construct a phylogenetic tree by the neighbor-joining (NJ) method. Transmembrane domains were predicted using a program for the prediction of transmembrane helices in proteins "TMHMM Server v2.0" (http://www.cbs.dtu.dk/services/TMHMM-2.0/).

2.4. Reverse transcription (RT)-PCR for tissue distribution

Dorsal skin, caudal fin, and head kidney tissue were taken from three goldfish. A sample of RNA was prepared using Isogen (Nippon Gene). RNA was then treated with TURBO DNase (Ambion, Austin, TX, USA) for 4 h at 37 °C. RNA yield was estimated by spectrophotometry. For each tissue, an equal amount of total RNA (100 ng) from three individuals was combined and subjected to amplification using a One-Step RT-PCR kit (Qiagen) with primer sets shown in Table 2. *β-actin* cDNA was used as a positive control. PCR products were electrophoresed on 3% agarose gel (Agarose S, Nippon Gene) and visualized with 0.025% ethidium bromide. Photographs were taken using a Densitograph (Atto, Tokyo, Japan).

Table 1
Custom oligonucleotide primers used for PCR to amplify cDNA fragments of goldfish *Mc1r*, *2r*, and *3r*.

Primer	Target	Nucleotide sequence
MC1-fw1	MC1R	5′-ATG (TC)TA CTG A(CA)G GA(GC) CAT GG-3′
MC1-rv1	MC1R	5′-(GT)GC TGA A(AG)T AGC ACT TGC AG-3′
GSP-MC1-fw1	MC1R	5′-CGT CAC GTT TTT TGG CTT GA-3′
GSP-MC1-rv1	MC1R	5′-GGA AAC GAC GGA ACT GCA TA-3′
GSP-MC1-fw2	MC1R	5′-GTC AAA GGT GTG CTG AAG GA-3′
GSP-MC1-rv2	MC1R	5′-CAA CGC AGA TGC TCC TTA AG-3′
MC2-fw1	MC2R	5′-AC(TA) GAC TGC GCT GAG GTC CA-3′
MC2-rv1	MC2R	5′-CAC ATG CAG AGT AGA GAG TC-3
MC2-fw2	MC2R	5′-GTT GTT TAA AGA CGC CGG AC-3′
MC2-rv2	MC2R	5′-GAG TGA (AG)CG GTA GCA (TC)TC AC-3′
GSP-MC2-fw1	MC2R	5′TTG ATT GGG GTG TTT GTG GC-3′
GSP-MC2-rv1	MC2R	5′CTT GAT GTC GGC TAG GAT CA-3′
GSP-MC2-fw2	MC2R	5′CCA GAC TCA TGT CTC TGA GA-3′
GSP-MC2-rv2	MC2R	5′-GTG AAG CAT GTA TTG CTG GG-3′
MC3-fw1	MC3R	5′-TAT GTG ACG AGG TCC (AC)(AG)A T(CT)C A-3′
MC3-rv1	MC3R	5′-AG(AG) A(CT)C AGG TAT GTG (GT)TG AA(AG)-3′
GSP-MC3-fw1	MC3R	5′-CCA CCT CAT TCT GCT GGT GT-3′
GSP-MC3-rv1	MC3R	5′-CCA AGA TGA CGA GGA TGT TC-3′
GSP-MC3-fw2	MC3R	5′-CAG TCC ACC ATC TGA ATC AG-3′
GSP-MC3-rv2	MC3R	5′-ACC ACC ATG CTT TGG CAT CT-3′
UPM	MC1R, 2R,3R	5′-CTA ATA CGA CTC ACT ATA GGG CAA GCA GTG GTA TCA ACG CAG AGT -3′

Synthesis of primers was performed by Nihon Gene Research Lab. (Sendai, Japan).

Table 2
Custom oligonucleotide primers used for tissue distribution of goldfish *Mcrs*.

Primer	Target	Nucleotide sequence
MC1-TD-fw1	MC1R	5′-GCT TGT CAC GGC AAA GAT GT-3′
MC1-TD-rv1	MC1R	5′-TGG CTT GTC GGC GAC TCT TA-3′
MC2-TD-fw1	MC2R	5′-ACA CCT GAA CGG TCG TTT CG-3′
MC2-TD-rv1	MC2R	5′-CTC AAG CCA CTT TGT CTC TG-3′
MC3-TD-fw1	MC3R	5′-TGT CTG TTC TTC CCC ATC TC-3′
MC3-TD-rv1	MC3R	5′-GGC GAT TGT TTA GTA CAG CA-3′
MC4-TD-fw1	MC4R	5′-TGC CTC CGA AAC GGT AGT GA-3′
MC4-TD-rv1	MC4R	5′-GCT GAT AAG GCA GAT GAG AA-3′
MC5-TD-fw1	MC5R	5′-CTG TCA CTT TGG GCC ATC AG-3′
MC5-TD-rv1	MC5R	5′-TCT GAT GAA ATG GTC CTC CA-3′

Synthesis of primers was performed by Nihon Gene Research Lab. (Sendai, Japan).

2.5. Skin cell dispersion and RT-PCR

Skin cell dispersion was performed as described previously [26,27]. Small parts of caudal fin or dorsal skin were rinsed in Hanks' balanced salt solution (HBSS). The samples were allowed to stand for 20 min at room temperature in a dissociation medium [DM: 1 mg/mL collagenase type III (Worthington, Freehold, NJ, USA), 1×10^{-4} M epinephrine (Sigma–Aldrich, St. Louis, MO, USA), 2 mg/mL bovine serum albumin (Sigma–Aldrich), 0.1 mg/mL soybean trypsin inhibitor (Roche, Indianapolis, IN, USA), and 5 U/mL DNase I (Takara)] and then gently agitated for 10 min in the same solution. The DM was removed, and the samples were rinsed three times with HBSS. Finally, during the gentle agitation in fresh DM, dispersed single xanthophores and other nonchromatophoric dermal cells were isolated using glass capillaries under a microscope. cDNA from an isolated cell was synthesized using the Super-Script III CellsDirect cDNA Synthesis System (Invitrogen, Carlsbad, CA, USA), according to the manufacturer's instructions. The cDNA obtained from three cells was dissolved in 90 μL H_2O, and a 5-μL aliquot was analyzed using PCR to detect *Mcr* mRNAs. As a control, 2 μL was analyzed to detect *β-actin* mRNA. The primer sets for *Mcrs* and β-*actin* mRNA were the same as those used in Section 2.4. The PCR conditions programmed into the thermal cycler (MJ Mini; BIO-RAD) included reverse transcription at 50 °C for 50 min followed by amplification of the appropriate cDNA fragment with activation of the enzyme at 95 °C for 15 min followed by 40 cycles of (i) denaturation for 15 s at 94 °C, (ii) annealing for 30 s at 60 °C, and (iii) extension for 40 s at 72 °C. The PCR products were electrophoresed and visualized as described above. The series of experiments from cell dispersion to PCR was repeated three times.

2.6. Incubation of fish scales with MC peptides for measurements of pigment-dispersing activities

Scales removed from the dorsal skin were incubated in HBSS for 1 h at 20 °C. After changing HBSS, the scales were incubated under the same conditions. Subsequently, the scales were incubated in HBSS containing serially diluted MSH at final concentration of 1 nM to 1 μM for 1 h. Photographs were taken using a light microscope equipped with a digital still camera (PDMCII, Olympus, Japan), and subsequently ten randomly selected xanthophores from five skin parts were observed for each peptide concentration. The xanthophore index (XI) was calculated to evaluate the pigment-dispersing activity of each peptide by analogy with melanophore index [12]. An average XI obtained from 10 xanthophores represented XI of each skin part ($n = 5$).

2.7. Incubation of head kidney parts with MC peptides for measuring cortisol-releasing activities

L-15 medium was used for incubation. The washing and incubation temperature was 20 °C. Head kidney tissues dissected from several goldfish were diced to approximately 1 mm^3 and combined. A flask containing the diced tissue (1 g/100 mL) was incubated for 30 min with occasional shaking. This incubation for washing was repeated three times and the medium was exchanged at the end of each incubation period. Following the transfer of approximately 20 mg of the diced tissues to each well of a 48-well plate, the tissue was preincubated for 90 min in 0.5 mL medium. After changing the medium, the tissue was incubated for an additional 60 min in 0.5 mL medium containing MC peptides ($ACTH_{1-24}$, Des-Ac-α-MSH, α-MSH, or Di-Ac-α-MSH). Final concentrations ranged from 10 to 100 nM. Control experiments were carried out for the same time periods without including hormone in the medium. Each assay was performed in duplicate ($n = 5$). Preincubation and incubation media were used for the cortisol assay. Cortisol levels after incubation were expressed as percentage of the levels